DIMENSIONALITY REDUCTION OF OPTICAL DATA: APPLICATION TO TOTAL OZONE COLUMN RETRIEVAL

Ana del Águila, Víctor Molina García, Dmitry S. Efremenko

Remote Sensing Technology Institute, German Aerospace Center (DLR),
Oberpfaffenhofen, Germany

ABSTRACT

The new generation of atmospheric composition sensors such as TROPOMI, deliver a great amount of data, which is recognized as Big Data. To process the challenging data volumes of spectral information, fast radiative transfer models (RTMs) are required. However, the bottleneck in remote sensing retrieval problems is the computation of the radiative transfer. Thus, the operational processing of remote sensing data requires high-performance RTMs for simulating spectral radiances (level-1 data). In particular, ozone total column retrieval algorithms use the level-1 data in the Huggins band (325-335 nm). Hence, accurate simulation of this absorption band may require several hundreds of monochromatic computations. However, hyper-spectral input data for RTMs has a redundant information, which can be excluded by using the dimensionality reduction techniques. In addition, there is a strong correlation between the input optical data for RTMs and output radiances. Such statistical dependency can be taken into account for accelerating level-1 data simulations using principal component analysis (PCA), thereby providing the performance enhancement for the whole processing chain. In this paper we analyze the efficiency and potential benefits of the optical data dimensionality reduction schemes for simulating the Huggins band and discuss several modifications of this approach.

Index Terms— PCA, data-driven algorithms, trace gas retrieval

1. INTRODUCTION

Atmospheric chemistry observations have received much attention in the last decades because they can improve our understanding of environmental issues such as climate change or stratospheric ozone depletion. In line with that objective, atmospheric composition sensors such as the TROPospheric Ozone Monitoring Instrument (TROPOMI), continuously measure the reflected spectral radiances to finally retrieve the trace gas concentrations. This new generation of sensors like the TROPOMI on board Copernicus Sentinel 5 Precursor (S5P) satellite, delivers challenging data volumes of spectral radiances (level-1 data) that require high-performance computing.

Radiative transfer models (RTMs) are an essential component of retrieval algorithms since they convert optical parameters of the atmosphere into spectral radiances. Usually, the computations of the spectral radiances at different wavelengths are independent and involve a computational loop over wavelengths, as shown in the following pseudo-code:

```
for each wavelength:
      radiance[wavelength] = RT_solver(
          wavelength);
```

However, this line-by-line methodology described in the above code is computationally expensive and inefficient in hyper-spectral remote sensing retrieval applications. This motivates the need for a fast and accurate technique to minimize the spectral mapping computational time. In this regard, Natraj et al. [1] proposed to reduce the dimensionality of the input data due to the strong correlation between atmospheric optical data in the spectral channels by means of an acceleration technique based on the principal component analysis (PCA) to reduce the number of calls to RTMs. To this end, the predictor-corrector approach is proposed as a new method to enhance the performance of the computation of the radiative spectrum for simulating the level-1 data. The predictor stands for a fast approximate radiative transfer model which gives a first estimation for the radiance spectrum. The corrector can be regarded as a post-processing step, in which a correction for the predictor is derived taking into account the redundancy in the input data.

This paper focuses on the reflected spectra of solar radiation in the Huggins band (325-335 nm) that is used to retrieve the total ozone column. The aim of the present work is to evaluate the efficiency of the dimensionality reduction technique of optical parameters in the Hartley-Huggings band regarding the acceleration techniques based on PCA.

2. INPUT DATA STRUCTURE: PRINCIPAL COMPONENT ANALYSIS

The atmospheric state is characterized by the state vector $\mathbf{x}_w$ which consists of a set of optical thickness and single scattering albedo values. For a set of input data vectors

doi:10.2760/848593

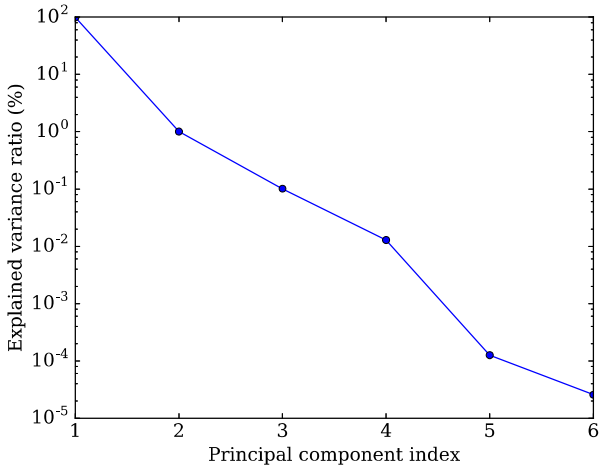

Fig. 1. Explained variance ratio vs. principal component index for the Huggins band simulation.

$\{\mathbf{x}_w\}_{w=1}^W$, where $\mathbf{x}_w \in \mathbb{R}^N$, the mean vector is defined as $\bar{\mathbf{x}} = (1/W)\sum_{w=1}^W \mathbf{x}_w$ and W is the number of spectral points. By using the principal component analysis, the vector $\mathbf{x}_w$ is represented in a new basis $\{\mathbf{q}_k\}_{k=1}^M$ of reduced dimensionality, namely,

$$\mathbf{x}_w \approx \bar{\mathbf{x}} + \sum_{k=1}^{M} y_{wk}\mathbf{q}_k = \bar{\mathbf{x}} + \mathbf{Q}\mathbf{y}_w, \quad w = 1, \ldots, W, \quad (1)$$

where $\mathbf{Q} = [\mathbf{q}_k]_{k=1}^M$ are the matrices of dimension $N \times M$, with columns $\mathbf{q}_k$; y_{wk} is the k-th element of $\mathbf{y}_w \in \mathbb{R}^M$ and N is the $N-$dimensional vector considering a discretization of the atmosphere in L layers, $N = 2L+1$. In the classical principal component analysis (PCA) the basic vectors $[\mathbf{q}_k]_{k=1}^M$ are taken as the eigenvectors of the covariance matrix of vectors $\mathbf{x}_w$.

Figure 1 shows the ratio of explained variance depending on the indexes of principal component scores (PCSs), for the input optical data in the Huggins band. The amount of explained variance for the first and second principal component is 98.88 % and 1.00 %, respectively. Thus, not more than two PCSs are sufficient to represent the input data.

3. FAST PREDICTOR MODELS

The fast predictor models consist of radiative transfer models used to compute the radiance as a first estimator. The radiative transfer models used in this study are the multi-stream model, the two-stream model (TS), the single-scattering model (SS) and the model based on the weak absorption Beer-Lambert law. In SS, multiple scattering events are neglected. The multi-stream RTM is based on the discrete ordinate method with matrix exponential (DOME) [2, 3], and uses 16 streams. In the current study, this model is considered as the exact model. Note, that the TS RTM is a two-stream version of DOME, in which the eigenvalues and the eigenvectors of the layer matrix are computed analytically [4]. Essentially, the SS and the Beer-Lambert (BL) models are wrong and directly not applicable for modeling the reflection function in the UV region. However, their results can be correlated with the exact solution and, therefore, can be improved by applying an appropriate corrector.

4. CORRECTION IN THE REDUCED DATA SPACE

We define a correction function $f(\lambda, \boldsymbol{\xi})$ as

$$f(\lambda, \boldsymbol{\xi}) = \ln \frac{L(\lambda, \boldsymbol{\xi})}{L^{\mathrm{P}}(\lambda, \boldsymbol{\xi})}, \quad (2)$$

here $\boldsymbol{\xi}$ is the state vector of input parameters (practically, a set of monochromatic optical data), L^{P} is the radiance provided by the predictor, $L(\lambda, \boldsymbol{\xi})$ is the radiance simulated by the exact model.

Introducing $\Delta\mathbf{x}_w = \sum_{k=1}^M y_{wk}\mathbf{q}_k$, we consider the Taylor expansion of $f(\mathbf{x}_w)$ around $\bar{\mathbf{x}}$:

$$\begin{aligned} &f(\mathbf{x}_w) \approx f(\bar{\mathbf{x}} + \Delta\mathbf{x}_w) \approx \\ &f(\bar{\mathbf{x}}) + \Delta\mathbf{x}_w^T \nabla f(\bar{\mathbf{x}}) + \frac{1}{2}\Delta\mathbf{x}_w^T \nabla^2 f(\bar{\mathbf{x}})\,\Delta\mathbf{x}_w, \end{aligned} \quad (3)$$

where ∇f and $\nabla^2 f$ are the gradient and Hessian f, respectively. Note, that to estimate them in the initial data space, one would require $N+1$ forward calls for ∇f and N^2+1 forward calls for $\nabla^2 f$. The key point is that the second and third terms in Eq. (3) are estimated in the reduced data space using the formulas of central differences, from which after simplifications, we get

$$\begin{aligned} f(\mathbf{x}_w) \approx & f(\bar{\mathbf{x}}) + \frac{1}{2}\sum_{k=1}^{M}\left(f_k^+ - f_k^-\right) y_{wk} \\ &+ \frac{1}{2}\sum_{k=1}^{M}\left(f_k^+ - 2f(\bar{\mathbf{x}}) + f_k^-\right) y_{wk}^2, \end{aligned} \quad (4)$$

where $f_k^{\pm} = f(\bar{\mathbf{x}} \pm \mathbf{q}_k)$.

Thus, the computations can be organized as shown in the following pseudo-code:

```
for each wavelength:
   approximate_radiance[wavelength] = predictor
       (wavelength);
for each principal_component:
      corrector[wavelength] = corrector(
          wavelength, principal_component);
```


doi:10.2760/848593

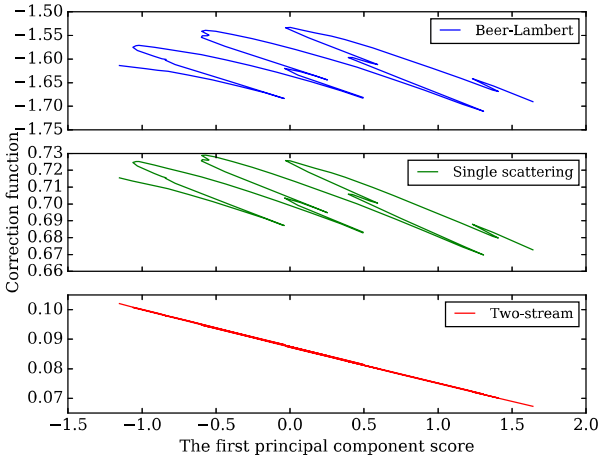

Fig. 2. Corrector vs the first principal component score.

5. PRACTICAL RESULTS

In this section, back-scatter measurements taken by the TROPOMI instrument in the Huggins band are simulated. The wavelength range is 325-335 nm containing W = 80. The atmosphere is discretized into 14 layers. The simulations are performed on a personal computer with RAM of 16 GB and processor Intel(R) Core(TM) i7-6700 CPU @ 3.40GHz.

Before proceeding further we analyze the behavior of the corrector as a function of principal component scores (PCS) of the input data. Figure 2 shows that the corrector for the TS model is highly correlated with the first PCS, and almost does not depend on the second PCS. Unlike TS, other predictor models remain correlation for the second PCS. Consequently, keeping one PCS (practically, setting M to 1 in Eq. 4), the computational time for the BL and SS models is reduced by factor of 2, however, at cost of significant lose in accuracy (about 5 times) with respect to the case when $M = 2$ PCSs are preserved. For the TS model, using just one PCS also reduces the computational time by factor of 2 without compromising the accuracy. Thus, for further analysis we set $M = 1$ for the TS model and $M = 2$ for SS and BL models.

In addition, we note, that the dependence of the corrector function is more linear when the TS model is used as predictor. Therefore, the computations of the second order derivatives can be skipped and the last term in Eq. 4 can be neglected. For other models, the dependence is nonlinear and require computations of both the first and second derivatives.

With this setup, in the next section we examine the accuracy and the computational time of the predictor-corrector approach.

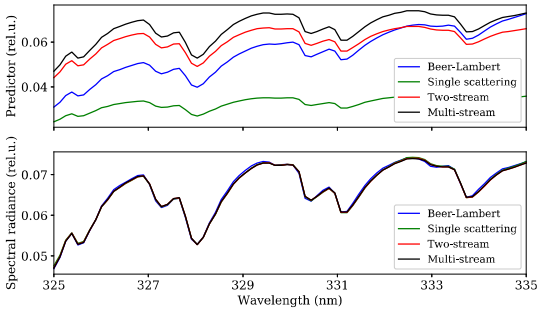

Fig. 3. (upper panel) spectral radiance computed by the predictors; (bottom panel) spectra after applying the corrector.

5.1. Computational time

Table 1 shows the computational time for the models. The computational time required for evaluating the predictor is minimal for the BL model, while it is maximal for the TS model. Such behavior is expected since the BL model is a simplified model (its performance is limited by I/O interfaces).

However, for the corrector function, the results are comparable. The setup, discussed in the previous section, makes the differences even smaller. As a result, the total computational time differs by factor less than two. The PCA requires $\sim$ 0.00075 s for all cases. Note, that the computational time for the exact model is $\sim$ 5.5 s. Thus, the predictor-corrector approach provides the performance enhancement of about 6-10 times, depending on the model used for the predictor. During clear-sky conditions, all computational times are reduced due to the lower number of coefficients in the phase function.

5.2. Accuracy

Table 2 shows the mean and maximum errors in percentage for the three models studied in this paper. The mean relative error for the BL and SS corrected are 83 % and 67 % higher than the TS corrected model, respectively. The similar behavior is also observed for the maximum error, which is lower for the TS followed by SS and finally BL model.

Figure 3 shows the spectral radiances computed by using the predictor models (upper panel) and those after applying the correction function (bottom panel) (all spectra are normalized by the solar irradiance). It can be observed that the higher differences with the exact model are for the BL model followed by the SS and TS models. This result is expected since the BL model is a simplified model and then, the errors are higher. Also, the TS model is a particular case of the exact model with two discrete ordinates, therefore, the higher accuracy is expected. At the same time, the accuracy of the BL model (which is essentially wrong) is significantly improved

doi:10.2760/848593

Table 1. Computational time for the processes: radiance predicted, radiance corrected and the total time for each model

Predictor model	Computational time (sec)			Acceleration factor
	Predictor	Corrector	Total	
Beer-Lambert	$47 \cdot 10^{-6} \pm 5 \cdot 10^{-6}$	0.470 ± 0.008	0.471 ± 0.008	11.7
Single scattering	0.212 ± 0.008	0.521 ± 0.010	0.734 ± 0.012	7.5
Two-stream	0.531 ± 0.013	0.360 ± 0.012	0.892 ± 0.020	6.2

Table 2. Mean and maximum error for the three predictor models

	BL	SS	TS
Mean error (%)	0.41	0.21	0.07
Max. error (%)	0.87	1.2	0.21

by the correction procedure. This illustrates that the information about the 'exact' spectral radiance is contained in the optical data and can be retrieved by using learning algorithms. In this context, the predictor-corrector algorithm can be considered as a specific machine learning algorithm. But unlike classical machine learning, here we are confronted with the *ad hoc* learning, i.e. the algorithm extracts the most informative part from the data and predicts the correct behavior using the computations in the reduced data space.

6. CONCLUSIONS

Efficiency of the predictor-corrector procedures together with the dimensionality reduction technique has been analyzed for radiance spectra simulations in the Huggins band. The predictor is used to compute the first guess for the exact radiance. Three predictors based on the two-stream model, the single scattering model and the Beer-Lambert absorption law have been included in the computations. The corrector is a function which improves the accuracy of the approximate models. It is computed in the reduced data space, in which the difference between the exact model and the approximate model is estimated. As the input data is reduced, the behavior of the corrector is easily pronounced and therefore can be approximated by a low degree polynomial. Overall, the total performance enhancement due to dimensionality reduction is about one order of magnitude. As shown in [5], the presented approach can be differentiated as a whole or applied directly for differentiated radiances for computing Jacobian matrix in the efficient manner.

It has been shown that two principal components are sufficient to represent the input optical data. For the two-stream model, the corrector is highly correlated with the first principal component, and this dependence is almost linear. That allows to use in the computations only one principal component and the first order Taylor expansion in estimating the correction function. Thus, the results presented in [5] can be improved by reducing number of principal components and computing the correction function only with first order Taylor expansion. Other predictors considered in the paper require two principal components and the second order Taylor expansion. No obviously superior method has emerged in our bench-marking studies (increasingly time-consuming predictors require more sophisticated correctors, and vice versa). However, the best accuracy is obtained with the two-stream model as a predictor. We plan to analise efficiency of the described approach in the framework of GPU computations.

Acknowledgements

This work was funded by the DLR/DAAD Research Fellowships 2018 and 2015 (grants no. 57424731 and 57186656), organized by the German Academic Exchange Service (DAAD) and the German Aerospace Center (DLR).

REFERENCES

[1] V. Natraj, R. Shia, and Y.L. Yung. On the use of principal component analysis to speed up radiative transfer calculations. *J Quant Spectrosc Radiat Transfer*, 111(5):810–816, 2010. doi: 10.1016/j.jqsrt.2009.11.004.

[2] A. Doicu and T. Trautmann. Discrete-ordinate method with matrix exponential for a pseudo-spherical atmosphere: Scalar case. *J Quant Spectrosc Radiat Transfer*, 110(1-2):146–158, 2009. doi: 10.1016/j.jqsrt.2008.09.014.

[3] V. Molina García, S. Sasi, D.S. Efremenko, A.Doicu, and D.Loyola. Radiative transfer models for retrieval of cloud parameters from EPIC/DSCOVR measurements. *J Quant Spectrosc Radiat Transfer*, 213:228–240, 2018. doi: 10.1016/j.jqsrt.2018.03.014.

[4] R. Spurr and V. Natraj. A linearized two-stream radiative transfer code for fast approximation of multiple-scatter fields. *J Quant Spectrosc Radiat Transfer*, 112(16):2630–2637, 2011. doi: 10.1016/j.jqsrt.2011.06.014.

[5] D.S. Efremenko, A. Doicu, D. Loyola, and T. Trautmann. Optical property dimensionality reduction techniques for accelerated radiative transfer performance: Application to remote sensing total ozone retrievals. *J Quant Spectrosc Radiat Transfer*, 133: 128–135, 2014. doi: 10.1016/j.jqsrt.2013.07.023.